

Radial Turbine with Pitch-controlled Guide Vanes for Wave Energy Conversion

M. Takao¹, M. Suzuki², T. Setoguchi³, B. Pereiras⁴ and F. Castro⁵

¹ Department of Mechanical Engineering,
Matsue College of Technology,
14-4 Noshikuma-cho, Matsue-shi, Shimane 690-8518, Japan
E-mail: takao@matsue-ct.jp

² Department of Mechanical Engineering,
The University of Tokyo,
7-3-1 Hongo, Bunkyo-ku, Tokyo 113-0033, Japan
E-mail: wells@cfdl.t.u-tokyo.ac.jp

³ Institute of Ocean Energy,
Saga University,
1 Honjo-machi, Saga-shi, Saga 840-8502, Japan
E-mail: setoguci@me.saga-u.ac.jp

⁴ Energetic Engineering and Fluids Mechanics Department,
University of Valladolid,
Paseo del Cauce, s/n. E-47011, Valladolid, Spain
E-mail: brunopereiras@eis.uva.es

⁵ Energetic Engineering and Fluids Mechanics Department,
University of Valladolid,
Paseo del Cauce, s/n. E-47011, Valladolid, Spain
E-mail: castro@eis.uva.es

Abstract

A radial turbine with pitch-controlled guide vanes has been proposed and investigated experimentally by model testing, in order to develop a high performance radial turbine for wave energy conversion. However, according to previous studies, it was clarified that the turbine efficiency was not so high because the guide vane solidity was small. The objective of this study is to clarify the effect of guide vane solidity on the performance of this radial turbine and to enhance the turbine efficiency. As a result, the performance of the radial turbine with high solidity guide vane has been clarified under steady flow condition. Further, the performance of the radial turbine under unsteady flow condition has been clarified by using quasi-steady analysis.

Keywords: Ocean energy, wave energy conversion, radial turbine, pitch-controlled guide vane

Nomenclature

A flow passage area
 C_A input coefficient
 C_T torque coefficient

h height of flow path
 Q flow rate
 R mean radius of rotor
 t time
 T period of sinusoidal flow
 T_o torque
 U circumferential velocity of rotor
 v radial flow velocity under steady flow condition
 V maximum velocity of v under sinusoidal flow condition

Greek symbols

Δp pressure difference between settling chamber and atmosphere
 ϕ flow coefficient under steady flow condition
 Φ maximum value of ϕ under sinusoidal flow condition
 η efficiency
 η_p peak efficiency
 $\bar{\eta}$ mean efficiency
 θ setting angle of guide vane
 σ solidity of guide vane
 ω turbine angular velocity

Subscripts

d diffuser
 i inner guide vane
 n nozzle

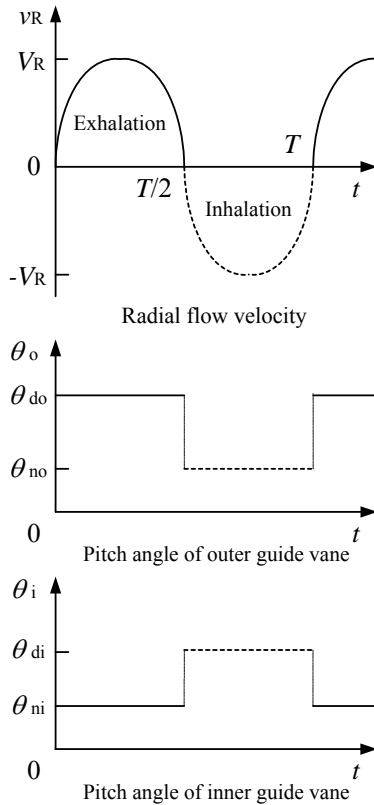


Figure 4: Behavior of pitch-controlled guide vanes.

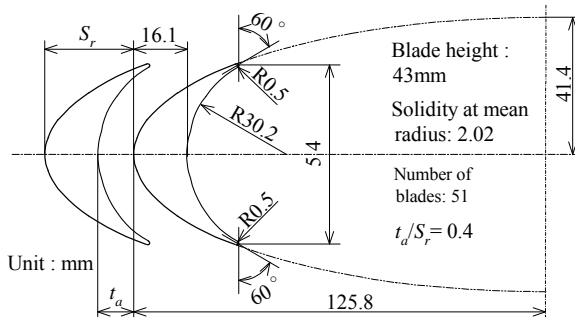


Figure 5: Rotor blade.

airflows (intermittently for short periods). The test turbine rotor shaft is coupled to the shaft of a servo-motor-generator through a torque transducer. The motor-generator is electronically controlled such that the turbine shaft angular velocity is held constant at any set value. The flow rate through the turbine Q , whether it is inhalation (flow from the atmosphere into the rig) or exhalation (flow from the rig to the atmosphere), is measured by Pitot tube survey. The radial flow velocity v_R at mean radius R in the turbine is calculated from $Q = A_R v_R$ where A_R is the flow passage area at mean radius ($= 2\pi R h$). In a typical test, for a particular turbine geometry, the volumetric flow rate Q , pressure difference between settling chamber and atmosphere Δp , turbine torque T_o and turbine angular velocity ω are all recorded. Thereby, data for one flow coefficient ϕ defined in Eq. (4) are obtained. Data for a range of flow coefficients are collected by varying flow rate or turbine angular velocity. Tests were performed with

turbine shaft angular velocities ω up to 68.1 rad/s and flow rates Q up to 0.275 m³/s.

The radial turbine shown in Fig. 1 was tested at a constant rotational speed under steady flow. The part of shroud casing and the part of disk covering the inner guide vane to the exit are flat and parallel to each other. The height of flow path of the turbine h (gap between the shroud casing and the disk) is 44 mm. The flow passage from inlet to inner guide vane entry has been shaped such that the flow area is constant along this passage. The turbine system has guide vanes before and behind the rotor so as to operate efficiently in a reciprocating airflow. They are set by pivots on the shroud casing wall as shown in Fig. 1. The guide vanes are controlled by the stepping motors, timing pulleys and timing belts. Each cascade of outer and inner guide vane changes the pitch angle simultaneously when the airflow direction changes. These guide vanes rotate between two angles, i.e., nozzle (upstream side guide vane of the rotor) setting angle θ_{ni} and diffuser (downstream one) setting angle θ_{di} in the case of inner guide vane and θ_{no} , and θ_{do} in the case of outer guide vane, as shown in Figs. 3 and 4, where V_R and T are the maximum velocity and period of sinusoidal airflow, respectively. However, the pitch angle is set at a particular value because tests are performed under steady flow conditions in the study.

The guide vane geometries are shown in Fig. 3. The guide vane consists of a straight line and circular arc. Details of the guide vanes are given by chord length of 50mm; solidity of outer guide vane of $\sigma_o=2.31$; solidity of inner guide vane of $\sigma_i=2.29$. The nozzle setting angle is only 15° for both the airflow direction, i.e., $\theta_{ni}=\theta_{no}=15^\circ$. In order to clarify the effect of the diffuser setting angle on the turbine characteristics, θ_{di} is from 20° to 60° for the inner guide vane in the case of inhalation, and θ_{do} from 30° to 90° for the outer guide vane in the case of exhalation.

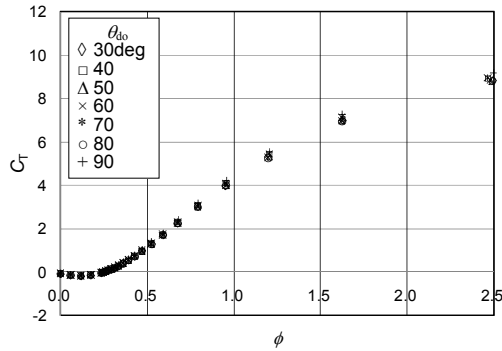
Rotor blade geometry is shown in Fig. 5 and is the same as what was used in previous studies [7]. The blade profile consists of a circular arc on the pressure side and part of an ellipse on the suction side. The ellipse has semi-major axis of 125.8mm and semi-minor axis of 41.4mm. The chord length and mean radius of rotor blade are 54 mm and $R=217.4$ mm.

3. Results and discussions

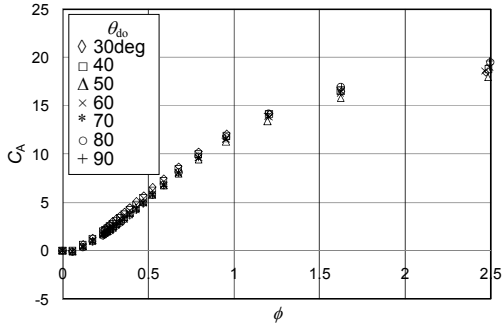
Experimental results on the running characteristics of turbine are expressed in terms of the torque coefficient C_T , input coefficient C_A and efficiency η , which are all plotted against the flow coefficient ϕ . The various definitions are

$$C_T = T / \{ \rho (v_r^2 + U_R^2) A_R r_R / 2 \} \quad (1)$$

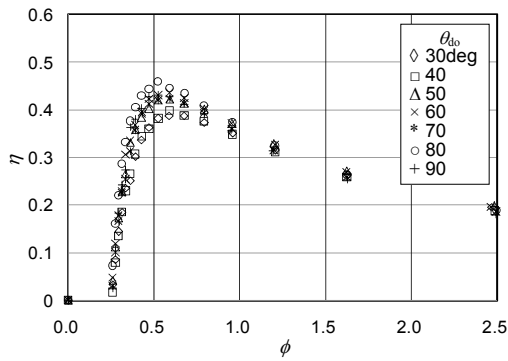
$$C_A = \Delta p Q / \{ \rho (v_R^2 + U_R^2) A_R v_R / 2 \} = \Delta p / \{ \rho (v_R^2 + U_R^2) / 2 \} \quad (2)$$



(a) Torque coefficient

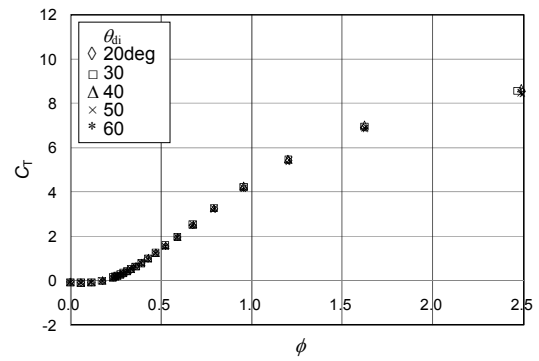


(b) Input coefficient

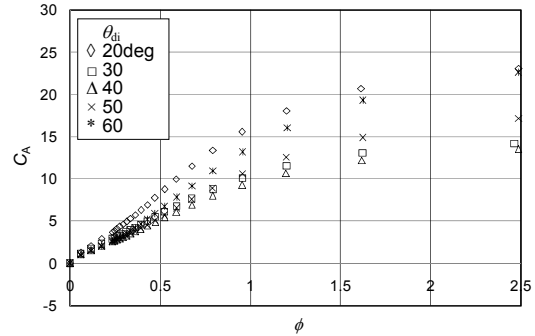


(c) Efficiency

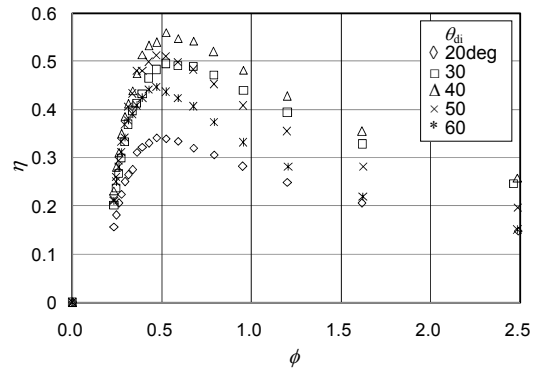
Figure 6: Effect of setting angle of outer guide vane on turbine characteristics (exhalation, $\theta_{ni}=15^\circ$)



(a) Torque coefficient



(b) Input coefficient



(c) Efficiency

Figure 8: Effect of setting angle of inner guide vane on turbine characteristics (inhalation, $\theta_{no}=15^\circ$)

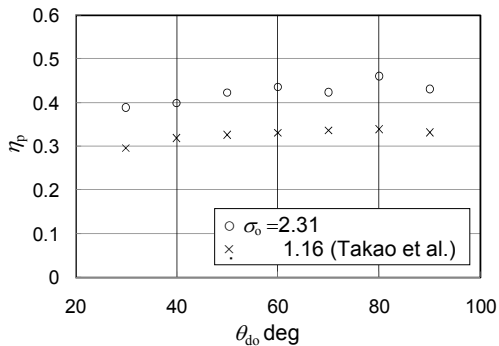


Figure 7: Effect of solidity and setting angle of outer guide vane on peak efficiency (exhalation, $\theta_{ni}=15^\circ$)

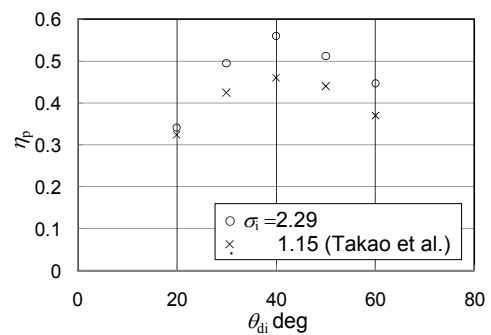


Figure 9: Effect of solidity and setting angle of inner guide vane on peak efficiency (inhalation, $\theta_{no}=15^\circ$)

where ρ , U_R and v_R are density of air, rotational speed at r_R and radial flow velocity at r_R , respectively. Efficiency, which is the ratio of shaft power output to

pneumatic power input, can be expressed in terms of the coefficients mentioned above:

$$\eta = T\omega / (\Delta p Q) = C_T / (C_A \phi) \quad (3)$$

The flow coefficient is defined as

$$\phi = v_R / U_R \quad (4)$$

Figures 6 to 9 show the effect of setting angle of the guide vane on the turbine characteristics under steady flow conditions. When the flow direction is from settling chamber to atmosphere (i.e. exhalation) the outer guide vane is downstream of the rotor and it works as a diffuser. Consequently, the torque coefficient C_T is independent of θ_{do} (Fig. 6a), whereas the input coefficient C_A decreases with increasing θ_{do} for $\theta_{do} \leq 50^\circ$ (Fig. 6b). It is evident from Figs. 6c and 7 that the peak efficiency η_p increases with θ_{do} for $\theta_{do} \leq 60^\circ$ and remains a stable situation at round 0.45. The highest efficiency occurs for $\theta_{do} = 80^\circ$ and its value is approximately 0.46. Moreover, it can be observed from Fig. 7 that the efficiency of the turbine with $\sigma_o = 2.31$ is higher than that of the turbine with $\sigma_o = 1.16$ [6] by 13 % in the case of $\theta_{do} = 80^\circ$. Conversely, when the flow direction is from atmosphere to chamber (i.e. inhalation), the inner guide vane is downstream of the rotor and it works as a diffuser. Hence, the torque coefficient C_T is independent of θ_{di} (Fig. 8a). Regarding $C_A - \phi$ characteristics, C_A decreases with increasing θ_{di} for $\theta_{di} \leq 40^\circ$ (Fig. 8b). The highest efficiency is obtained in the case of $\theta_{di} = 40^\circ$ and its value is approximately 0.56 (Figs. 8c and 9). Further, the efficiency of the turbine with $\sigma_i = 2.29$ is higher than that of the turbine with $\sigma_i = 1.15$ [6] by 11 % in the case of $\theta_{di} = 40^\circ$ (Fig. 9).

4. Turbine Characteristics under Sinusoidal Flow Conditions

Since the airflow into the turbine is generated by the OWC, it is very important to demonstrate the turbine characteristics under oscillating flow conditions. Here let us simulate the characteristics under sinusoidal flow conditions in order to clarify the effect of blade profile on the turbine characteristics. The steady flow characteristics of the turbine as shown in Figs. 6 and 8 are assumed to be valid for computing performance under unsteady flow conditions. Such a quasi-steady analysis has been validated by previous studies [8].

When the turbine is in the running conditions, the parameters such as T_o , ω , Δp and Q vary periodically in a sinusoidal oscillating flow. In this case, the turbine performances should be represented by mean value such as mean efficiency. The running characteristics of the turbine under sinusoidal flow conditions are evaluated by the mean efficiency $\bar{\eta}$ against the flow coefficient Φ , which are defined as follows:

$$\bar{\eta} = \left(\frac{1}{T} \int_0^T T_o \omega dt \right) / \left(\frac{1}{T} \int_0^T \Delta p Q dt \right) \quad (5)$$

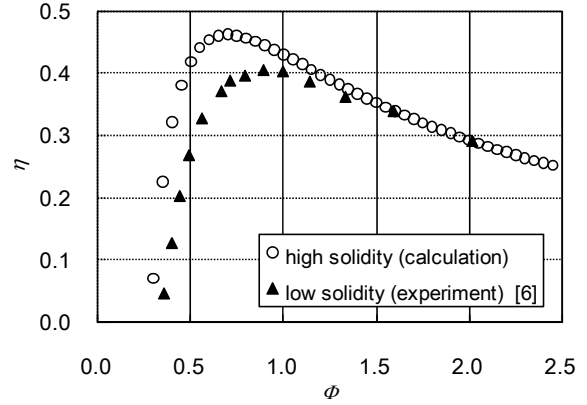


Figure 10: Effect of solidity of guide vane on mean efficiency under sinusoidal flow conditions

$$\Phi = V_R / U_R \quad (6)$$

Equation (5) can be rewritten in a dimensionless form as follows:

$$\bar{\eta} = \frac{\int_0^\Phi \{ C_T (1 + \phi^2) / \sqrt{\Phi^2 - \phi^2} \} d\phi}{\int_0^\Phi \{ C_A (1 + \phi^2) \phi / \sqrt{\Phi^2 - \phi^2} \} d\phi} \quad (7)$$

In the calculation, the flow coefficient under sinusoidal flow conditions is defined as:

$$\phi = \Phi \sin(2\pi t^*) \quad (8)$$

where t^* is dimensionless time ($=t/T$).

Figure 10 shows the effect of solidity of guide vanes on the mean efficiency under sinusoidal flow conditions. The circle symbols indicate the calculated result in the case of guide vane row with high solidity in this study ($\sigma_o = 2.31$, $\sigma_i = 2.29$, $\theta_{ni} = \theta_{no} = 15^\circ$, $\theta_{do} = 60^\circ$ and $\theta_{di} = 40^\circ$). The triangle symbol shows the experimental result in the case of guide vane row with low solidity in previous study ($\sigma_o = 1.16$, $\sigma_i = 1.15$, $\theta_{ni} = \theta_{no} = 15^\circ$, $\theta_{do} = 70^\circ$ and $\theta_{di} = 40^\circ$) [6]. As is evident from the figure, the efficiency in the case of guide vane with high solidity is higher than that of low solidity by approximately 0.06.

Therefore, it has been concluded from the above results that the performance of the radial turbine can be improved considerably by using guide vane row with high solidity.

5. Conclusions

In order to develop a high performance radial turbine for wave energy conversion, a radial turbine with pitch-controlled guide vanes has been investigated by model testing. Moreover, the effects of guide vane solidity and setting angle of the turbine performance have been clarified experimentally. As a result, the efficiency of turbine was improved by increase of guide vane solidity.

Acknowledgements

This study was performed under the Cooperative Research Program of IOES, Institute of Ocean Energy, Saga University (Accept# 09006D). The head author wishes to thank the IOES for their financial help in conducting the study.

References

- [1] K. Kaneko, T. Setoguchi, S. Raghunathan. (1992): Self-rectifying Turbines for Wave Energy Conversion. *International Journal of Offshore Polar Engineering*, Vol.2, No.3, pp.238-240.
- [2] M. E. McCormick, J. G. Rehak, B. D. Williams. (1992): An Experimental Study of a Bi-directional Radial Turbine for Pneumatic Energy Conversion. *Proceedings of Mastering Ocean through Technology*, Vol.2, pp.866-870.
- [3] M. E. McCormick, B. Cochran. (1993): A Performance Study of a Radial Turbine. *Proceedings of 1st European Wave Energy Conference*, pp. 443-448.
- [4] T. N. Veziroglu (editor). (1985): 'Alternative Energy Sources VI, Vol. 3, Wind/Ocean/Nuclear/Hydrogen', *Hemisphere Publishing Corporation*, pp. 169-181.
- [5] Setoguchi, T., Santhakumar, S., Takao, M., Kim, T. H., Kaneko, K., 2002, "A Performance Study of a Radial Turbine for Wave Energy Conversion", *Journal of Power and Energy*, Vol. 216, No. A1, pp. 15-22.
- [6] M. Takao, Y. Fujioka and T. Setoguchi. (2005): Effect of Pitch-Controlled Guide Vanes on the Performance of a Radial Turbine. *Ocean Engineering*, Vol. 32, No. 17-18, pp. 2079-2087.
- [7] T. Setoguchi, M. Takao, Y. Kinoue, K. Kaneko, S. Santhakumar, M. Inoue. (2000): Study on an Impulse Turbine for Wave Energy Conversion. *International Journal of Offshore Polar Engineering*, Vol.10, No.2, pp. 145-152.
- [8] M. Inoue, K. Kaneko, T. Setoguchi, S. Raghunathan, (1986): Simulation of Starting Characteristics of the Wells Turbine. *Proceedings of AIAA/ASME 4th Fluid Mechanics and Plasma Dynamic Laser Conference*, AIAA-86-1122.